CCC Annual Report

UIUC, August 14, 2013

Prediction, Measurement, and Optimization of Mold Fluid Flow in Continuous Slab Casting with FC Mold at Baosteel

Kai Jin and B.G. Thomas

Department of Mechanical Science & Engineering
University of Illinois at Urbana-Champaign

Overall Objectives

- Improve understanding of fluid flow in the Baosteel slab-casting mold, including the effect of EMBr;
- Develop off-line CFD model to accurately model multiphase fluid flow with EMBr (prediction of flow pattern, surface velocity, etc.) and validate model by comparing with measurements at Baosteel: nailboard velocity, and bubble entrapment location;
- Study Ar gas bubble behavior: predict bubble trajectories and entrapment;
- Investigate effect of EMBr, Ar gas injection, submergence depth, SEN downward angle and casting speed on mold flow pattern and top surface velocity;
- Apply model to optimize EMBr operation in commercial slab casters, evaluate the quality of flow pattern and provide suggestions regarding operation;

Chapter 1 – Experiments
(Bubble entrapment measurements at Baosteel)

Methodology of Experiment
(Translation of Baosteel Bubble Summary Report[6])

- Casting Conditions as Table 1.
- Samples from **middle WF, ¼ WF** and **NF**, as shown in Fig. 1.
- Milling off steel layer by layer.
- Use 35x optical microscope to examine bubbles. Record bubble **number**, **distribution** and **size**.
- Examine from **3 mm beneath the outer surface,** after that grinded off **3 mm** each time until reached **12 mm**; change the grind step depth to **5 mm** and mill to **22 mm**. **6 layers** in total. Shown in Table 2.

Table 1 Casting Conditions

Casting speed (m/min)	Cross Section (mm)	EMBr FC	Upper port Ar injection (L/min)	Upper Plate Ar injection (L/min)	Submerged Port Ar injection (L/min)
1.2	230×1300	ON	25.9	7.8	4.1
		OFF	30.2	5.7	4.1
1.5	230×1250	OFF	39.2	6.7	4.1
		ON	39.2	6.7	4.1

Table 2 Sample Mill depth and Associated layer number

Mill/Grind Depth (mm)	Sample Layer Number
3	1
6	2
9	3
12	4
17	5
22	6

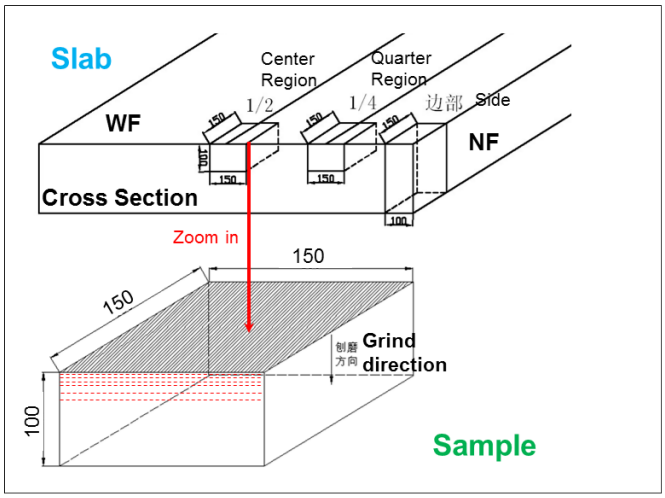

Experiment Result – Bubble Size (Translation of Baosteel Bubble Summary Report[6])

- In Experiment, observed bubble diameter range from ***0.05-1.45* mm**.
- **d_p < 0.1 mm, 57%**;
- **0.1mm < d_p<0.3mm 42.5%**;
- **dp > 1mm 0.5%** (2 bubbles, 1.45mm and 1mm)
- **2 bubbles larger than 1 mm. (1.45 mm and 1.00 mm)**. (observed in metallographic phase inclusion samples) casting conditions are listed in Table 3.
- Bubble size distribution shown in Table 4.

Table 3 Casting conditions for bubbles with diameter larger than 1mm

Bubble size	Casting speed	EMBr	Location	Distance From outer surface
1.45	1.5	OFF	side	<2mm
1	1.5	ON	side	<2mm

Table 4 Average bubble size and their location, μm

EMBr	Sample Layer	Casting Speed 1.2m/min Bubble Size (μm)			Casting Speed 1.5m/min Bubble Size (μm)		
		1/2	1/4	Side	1/2	1/4	Side
FC OFF	1	98.67	104.90	113.90	103.48	103.48	103.48
	2	97.33	106.40	136.60	126.50	111.60	72.50
	3	90.66	86.44	87.50	81.15	90.110	75.88
	4	77.46	92.48	99.60	92.92	91.30	96.80
	5	0	63.00	63.00	47.00	47.00	0
	6	0	0	0	0	0	70.50
FC ON	1	112.50	106.50	91.30	89.64	103.30	103.75
	2	96.80	100.00	110.00	134.15	122.16	106.25
	3	96.68	77.46	80.23	83.00	83.00	102.36
	4	85.37	66.40	99.60	80.62	88.53	89.22
	5	63.00	63.00	86.00	63.00	31.00	57.00
	6	109.00	63.00	47.00	63.00	63.00	0

Table 2 Sample Mill depth and Associated layer number

Mill/Grind Depth, mm	Sample Layer Number
3	1
6	2
9	3
12	4
17	5
22	6

Experiment Result: Plot of Average Bubble Size vs. Distance beneath Outer Surface (all in one plot)

1. Most larger bubbles (d_p>100 μm) are in layers 1 and 2 (3-6mm).
2. Most medium size bubbles (70 <d_p <100 μm) are found in layer 3 and 4 (8-12mm).
3. All small bubbles (d_p<70 μm) are found in layer 5 and 6.

- Entrapped bubble size decrease with depth.
- Large bubbles entrapped closer to meniscus. Fewer bubbles penetrate.
- In general, small bubbles can follow fluid flow and travel down. They were entrapped at lower position.

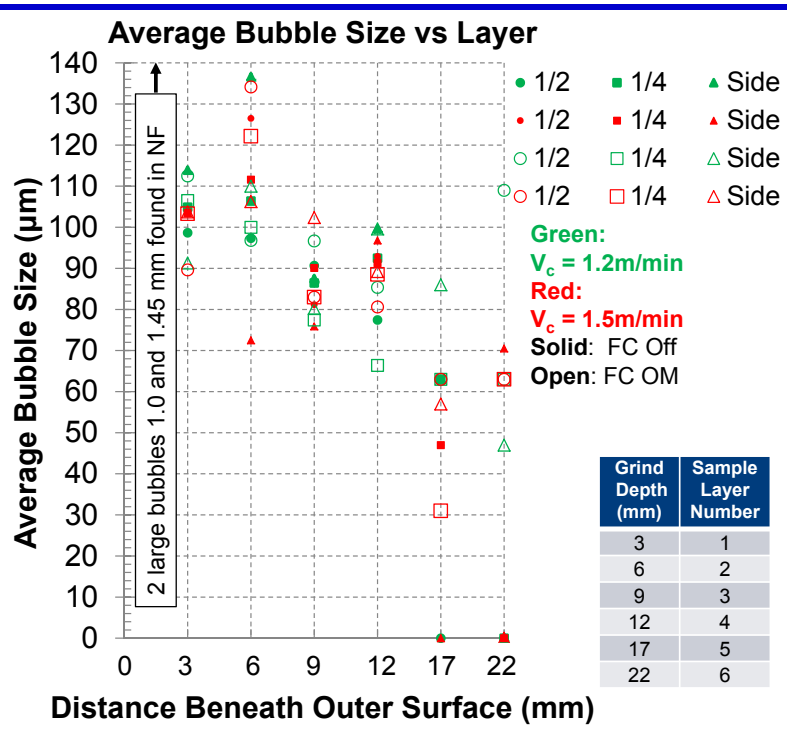

Grind Depth (mm)	Sample Layer Number
3	1
6	2
9	3
12	4
17	5
22	6

Experiment Result: Plot of Average Bubble Size vs. Distance beneath Outer Surface (Separate Plot)

Average bubble Size for different V_c (red-1.5 and 1.2-green m/s) at different sample location with different FC condition (FC ON-open marker and FC OFF-solid marker)

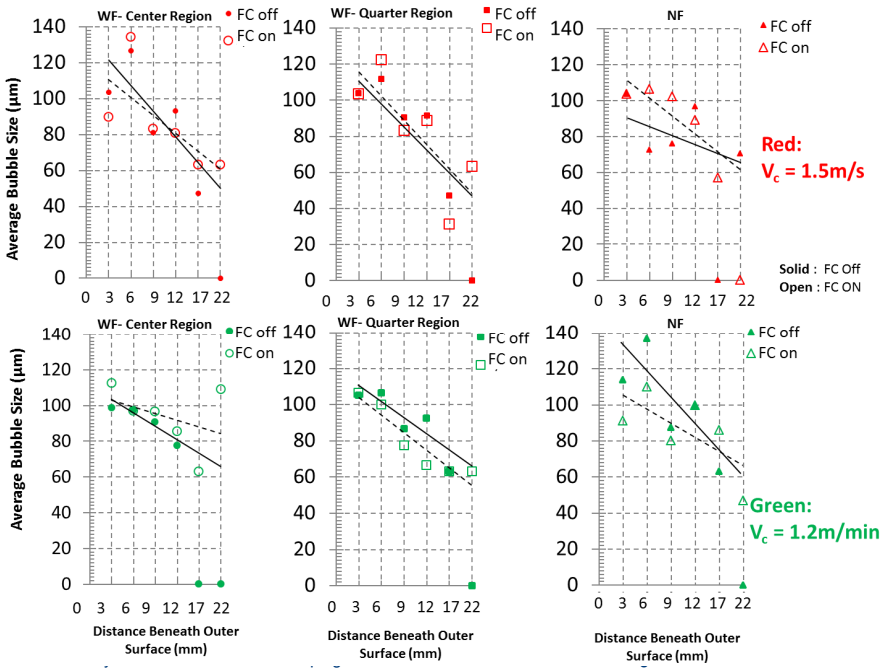

With higher casting speed (1.5m/s), the average bubble size is slightly smaller at a given depth.

But, considering the shell thickness is less at higher speed: bubble size is about the same with distance below meniscus (for different speeds).(Brian G. Thomas, Alex Dennisov, and Hua Bai)[11]

Results Summary: Bubble Number per 100cm² vs. Distance beneath Outer Surface

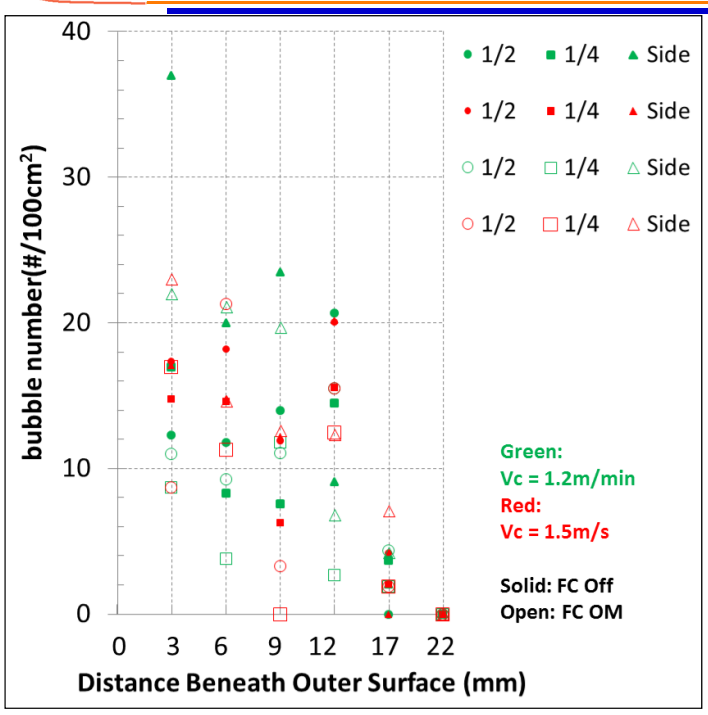

1. More bubbles are found in NF(side) than that in ½ and ¼ location. At the NF surface more bubbles are found in layer 1, 2 and 3, which is above 20 bubbles per 100cm².
2. Number of entrapped bubbles decreases with depth.
3. Fewer bubbles entrapped further below meniscus.
4. No bubble entrapped below mold exit.

Bubble Entrapment Depths at Inland

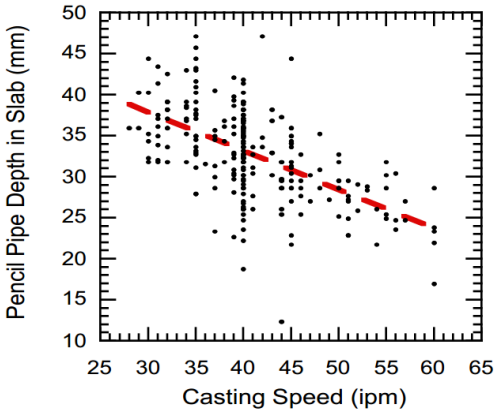

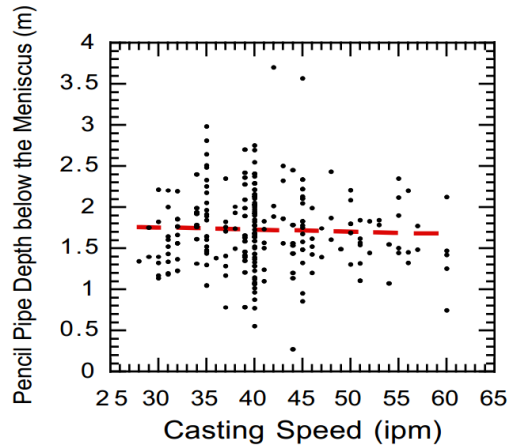

Casting speed vs. pencil pipe depth in slab and depth below meniscus
(Brian G. Thomas, Alex Dennisov, and Hua Bai, 1997 [14])

Two Larger Entrapped bubbles (diameter 70μm and 1.45mm)

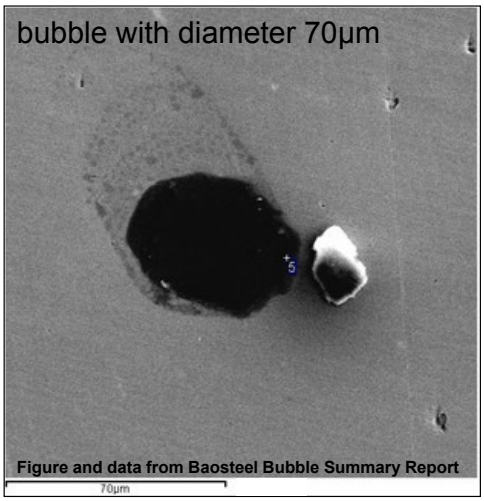

Chemical element	Weight%	Atom%
C K	26.30	44.42
O K	25.75	32.65
Al K	7.42	5.58
Si K	7.33	5.29
Fe K	33.19	12.06

Inclusion Al_2O_3 SiO_2

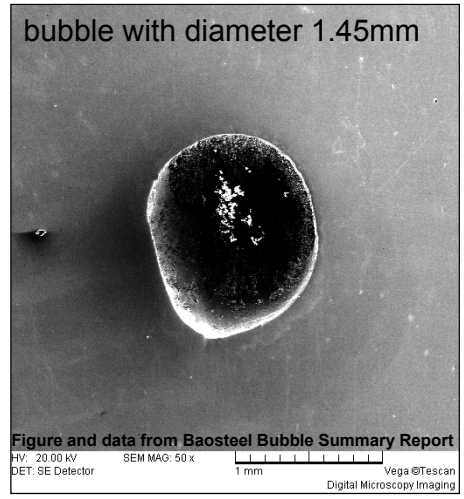

Chemical element	Weight%	Atom%
C K	18.94	38.89
O K	15.92	24.54
Al K	16.54	15.12
Fe K	48.59	21.46

Inclusion Al_2O_3

Chapter 2 – Simulation

Simulation Procedure

Two Steps

- A two-way coupled steady-state Eulerian-Lagrangian simulation (with k-ε model) was perform using FLUENT discrete phase model. This step is used to obtain the fluid field solution.

- Then, particles are injected into the domain and their trajectories are tracked. A stochastic model – Discrete Random Walk model is added to compensate the effect of turbulence dispersion of particles. There is no fluid iteration during this step.

Geometry and Boundary Conditions

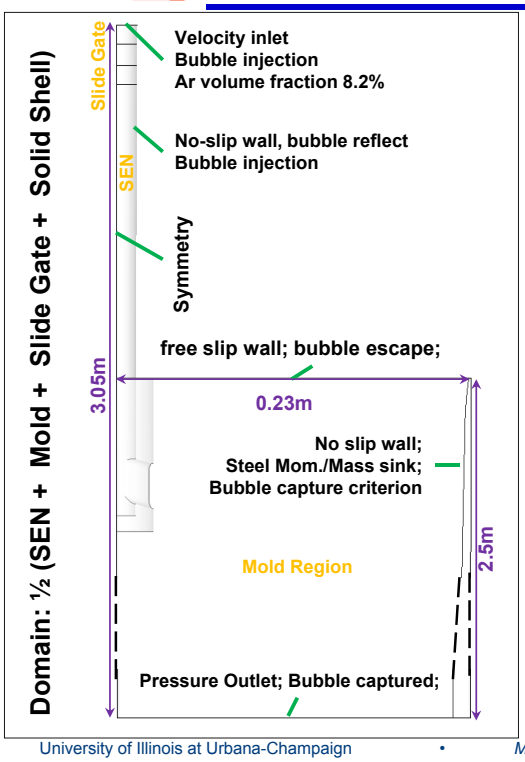

Casting Conditions

Casting Conditions	Value
Mold Thickness	230 mm
Mold Width	1300 mm
Submergence Depth	160 mm
Port Downward Angle	15 deg.
Casting Speed	1.5 m/min

Boundary Conditions

Location	Boundary Condition
Inlet	V = 1.69 m/s; 8.2% volume fraction of Ar
Outlet	pressure 184kpa; particle captured;
Symmetry Plane	Symmetry;
Meniscus	free-slip wall; particle escape;
NF and WF	no-slip wall; steel mass & momentum sink; particle capture criterion UDF;
SEN Walls	no-slip wall; particle reflect;

Solid Shell Model

- To avoid sharp shell tip, offset shell tip toward mold wall by 5mm.
- The **shaded parts** is the additional solid shell added into the domain.
- As a result, shell thickness at the region near the top surface is increased.
- Based on plant observation, shell thickness at the mold exit is around ***19 mm***, with casting speed 1.2 m/min.

$$S = k\sqrt{t}$$

$$L_{moldexit} = 0.8\ m \text{ and } S_{moldexit} = 19\ mm$$

$$V_c = 1.2 m/\min = 0.02\ m/s$$

$$t_{exit} = \frac{L_{moldexit}}{V_c} = \frac{0.8m}{0.02m/s} = 40\ s$$

$$k = \frac{S_{moldexit}}{\sqrt{t_{exit}}} = \frac{19mm}{\sqrt{40s}} = 3.00\ mm \cdot s^{-\frac{1}{2}} = 0.91\ \ inch \cdot \min^{-\frac{1}{2}}$$

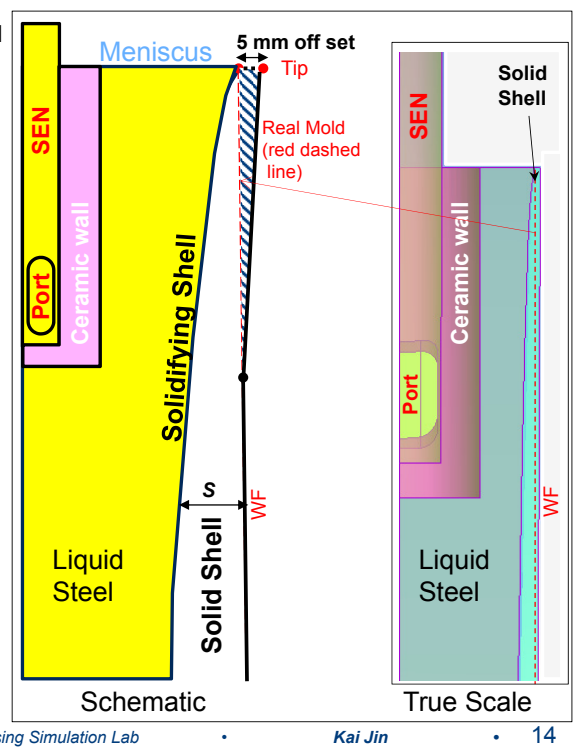

Mesh with Steel Shell in Domain
Structured hexahedron mesh created in ANSYS ICEMCFD
~1.2 million elements

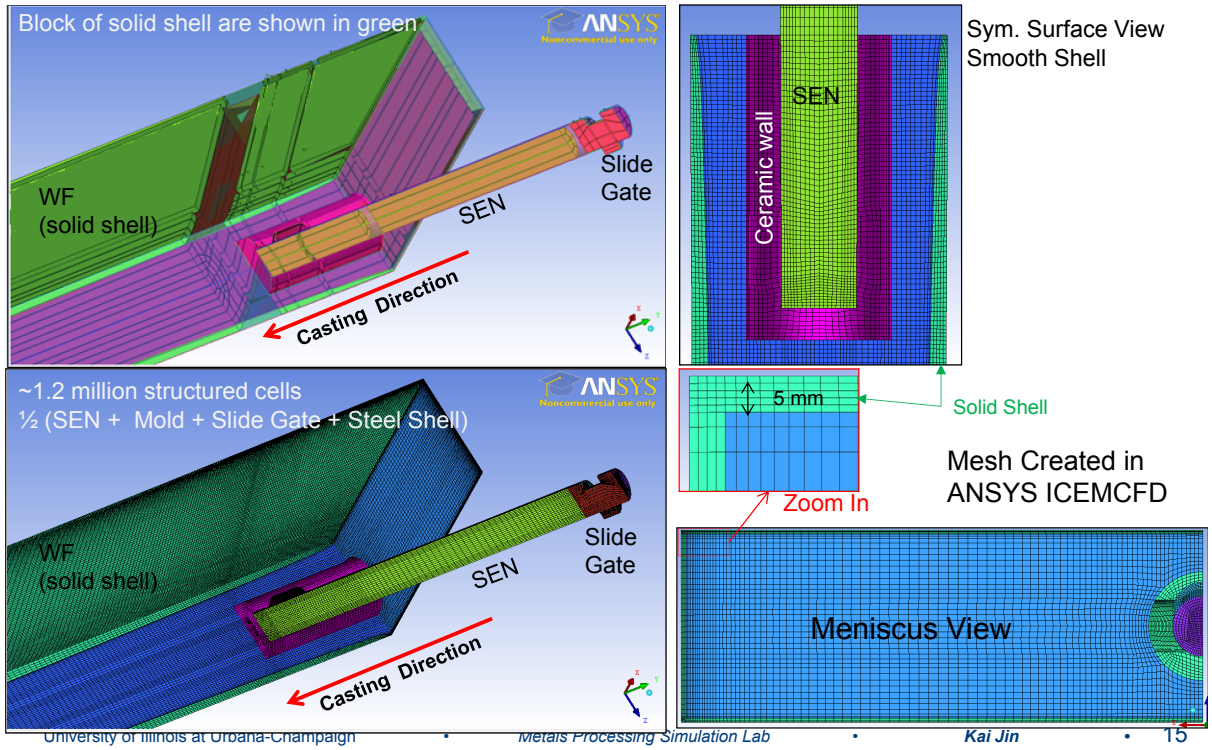

Governing Equation For Fluid Flow
Steel and Ar Properties

- Continuity Equation

$$\nabla \cdot (\rho \vec{u}) = 0$$

- Steel momentum equation

$$\rho \frac{\partial}{\partial t}(\vec{u}) + \rho \vec{u} \cdot \nabla \vec{u} = -\nabla p + \mu \nabla^2 \vec{u} + \vec{F}$$

Properties	Steel	Ar
Density (kg/m^3)	7,000	0.5
Viscosity (kg/m-s)	0.0063	2.12e-5
Electrical Conductivity (S/m)	714,000 [1]	1.0e-15 [2]
Magnetic Permeability (h/m)	1.26*10^{-6} [1]	4π*10^{-7}

- Steady-State RANS Turbulence Model (*k-ε*)

$$\frac{\partial}{\partial t}(\rho k) + \frac{\partial}{\partial x_i}(\rho k u_i) = \frac{\partial}{\partial x_j}\left[\left(\mu + \frac{\mu_t}{\sigma_k}\right)\frac{\partial k}{\partial x_j}\right] - \rho \overline{u'_i u'_j}\frac{\partial u_j}{\partial x_i} - \rho\epsilon; \qquad \mu_t = \rho C_\mu \frac{k^2}{\epsilon}$$

$$\frac{\partial}{\partial t}(\rho \epsilon) + \frac{\partial}{\partial x_i}(\rho \epsilon u_i) = \frac{\partial}{\partial x_j}\left[\left(\mu + \frac{\mu_t}{\sigma_\epsilon}\right)\frac{\partial \epsilon}{\partial x_j}\right] + C_{1\epsilon}\frac{\epsilon}{k}\left(\rho \overline{u'_i u'_j}\frac{\partial u_j}{\partial x_i}\right) - C_{2\epsilon}\rho\frac{\epsilon^2}{k}$$

$$C_{1\epsilon} = 1.44; \qquad C_{2\epsilon} = 1.92; \qquad C_\mu = 0.09; \qquad \sigma_k = 1.0\ ; \qquad \sigma_\epsilon = 1.3$$

$$\rho \overline{u'_i u'_j}\frac{\partial u_j}{\partial x_i} = \mu_t\left(\nabla \vec{u} + (\nabla \vec{u})^T\right) : \nabla \vec{u}$$

$\vec{u}$	Steel velocity
$\vec{g}$	Gravity
ρ	Steel density
$\vec{F}$	Sorce term
μ	Steel dynamic viscosity
k	Turbulent kinetic energy
ε	Turbulent dissipation rate

Particle Tracking with Random Walk Model

Equation of Motion for Particles

$$\frac{d\vec{u}_p}{dt} = F_D\left(\vec{u}-\vec{u}_p\right)+\frac{\vec{g}\left(\rho_p-\rho\right)}{\rho_p}+\vec{F}_s$$

$$\mathrm{Re}_p = \frac{\rho d_p\left|\vec{u}_p-\vec{u}\right|}{\mu}$$

$$F_D = \frac{18\mu}{\rho_p d_p^{\,2}}\frac{C_D\,\mathrm{Re}_p}{24}$$

Spherical drag law suggested by S. A. Morsi and A. J. Alexander

$$C_D = a_1+\frac{a_2}{\mathrm{Re}_p}+\frac{a_3}{\mathrm{Re}_p}$$

$$a_1,a_2,a_3=\begin{cases} 0,24,0 & 0<\mathrm{Re}_p<0.1 \\ 3.690,22.73,0.0903 & 0.1<\mathrm{Re}_p<1 \\ 1.222,29.1667,-3.8889 & 1<\mathrm{Re}_p<10 \\ 0.6167,46.50,-116.67 & 10<\mathrm{Re}_p<100 \\ 0.3644,98.33,-2778 & 100<\mathrm{Re}_p<1000 \\ 0.357,148.62,-47500 & 1000<\mathrm{Re}_p<5000 \\ 0.46,-490.546,578700 & 5000<\mathrm{Re}_p<10000 \\ 0.5191,-1662.5,5416700 & \mathrm{Re}_p>10000 \end{cases}$$

$\vec{u}_p$	Particle velocity
$\vec{u}$	Steel velocity
F_D	Drag force
$\vec{g}$	Gravity
ρ_p	Particle density
ρ	Steel density
$\vec{F}_s$	Sorce term
μ	Steel dynamic viscosity
d_p	Paticle diameter
C_D	Drag coefficient
Re_p	Particle Reynolds number
t_e	Eddy life time
τ	Particle relaxation time
t_{cross}	Eddy cross time
T_L	Fluid Lagrangian integral time
C_μ	Constant in k-ε model, 0.09
k	Turbulent kinetic energy
ε	Turbulent dissipation rate
$\dot{m}_p$	particle stream mass flow rate

Momentum Exchange to Fluid $\vec{F} = \sum\left(\frac{18\mu}{\rho_p d_p^{\,2}}\frac{C_D\,\mathrm{Re}_p}{24}\left(\vec{u}_p-\vec{u}\right)\right)\dot{m}_p\Delta t$

Discrete Random Walk Model

Gaussian distributed random velocity fluctuation, *u'*, *v'* and *w'* are generated from

$$u' = \zeta\sqrt{\overline{u'^2}} \qquad \sqrt{\overline{u'^2}}=\sqrt{\overline{v'^2}}=\sqrt{\overline{w'^2}}=\sqrt{2k/3}$$

ζ – standard normal distribution random number.

$$t_L = C_L\frac{k}{\epsilon}\approx 0.15\frac{k}{\epsilon}$$

$$\tau = \frac{\rho_p d_p^{\,2}}{18\mu} \qquad t_e = -t_L\ln(r) \qquad t_{cross} = -\tau\ln\left[1-\frac{C_\mu^{\,4/3}\frac{k^{3/2}}{\epsilon}}{\tau\left|\vec{u}-\vec{u}_p\right|}\right]$$

r – uniformly distributed random number from 0 and 1. This yields a random eddy life time.

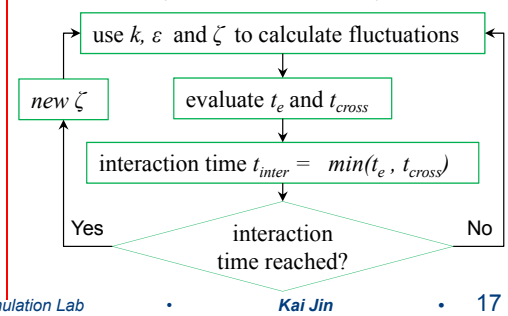

How Many Particles Should be Injected

Parameters	Values
Sample Length, Δz	*150mm*
Slab Thickness, L_y	*230mm*
Slab Width, L_x	*1300mm*
Total Ar Volume Fraction at SEN, α	*8.2%*
Volume of Ar injected in *half* of the caster when cast Δz length of slab, V_{Ar}	$2.0\times10^6 mm^3$

There are *10* different groups of bubbles and each group have the same diameter. Group *i* has diameter d_i, bubble number N_i and volume fraction α_i. *i = 1,2,…,10*. Then, the particle number of N_i satisfy the equation:

$$N_i = \frac{\alpha_i V_{Ar}}{\pi d_i^{\,3}/6} \qquad V_{Ar} = \frac{L_x L_y \Delta z}{1-\alpha}\alpha\cdot\frac{1}{2}$$

½ due to only half caster in computational domain

How to determine the value of α_i ?

Assume Ar bubble volume distribution satisfy the Rosin-Rammler distribution and the volume fraction of Ar contained in the bubbles which have diameter less than d_i is defined by $F(d_p)$.

$$F(d_i) = \frac{\begin{pmatrix}\text{Volume of all bubbles}\\ \text{with diameter} < d_i\end{pmatrix}}{\text{Volume of ALL bubbles}} = 1-\exp\left[-\left(\frac{d_i}{\bar{d}}\right)^b\right]$$

$\bar{d}$ mean bubble diameter, 3mm

b shape parameter, 4

$$\alpha_i = \begin{cases}\alpha\left[F(d_i)\right] & i=1\\ \alpha\left[F(d_i)-F(d_{i-1})\right] & i>1\end{cases}$$

Gas bubbles have diameter > 5mm have volume fraction ***1- F(5) = 0.04%***.

Gas bubbles have diameter < 1mm have volume fraction ***F(1) = 1%***.

Bubble Distribution

As stated before, there are **2 Steps** in the simulation:

1. Two-way coupled Eulerian-Lagrangian Simulation to obtain fluid field;
2. Particle are randomly released from inlet and the trajectories are tracked by using Random Walk Model.

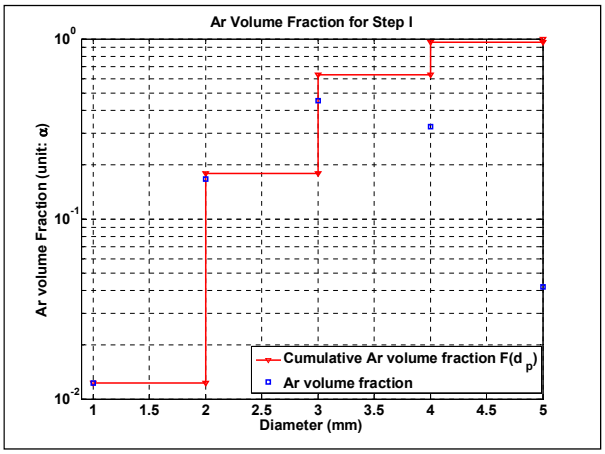

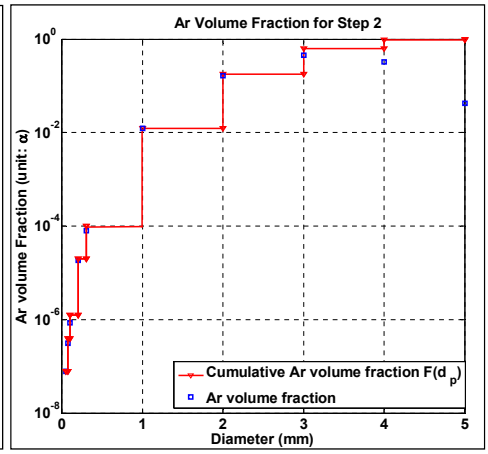

α is total Ar volume fraction at injection point whish is 8.2% in this case.

In step – 1, two-way coupled simulation with **5 different groups of bubbles** with diameter: 1, 2, 3, 4 and 5mm.

In step – 2, **10 different groups of bubbles** are injected and tracked with diameter: 0.05, 0.075, 0.1, 0.2, 0.3, 1, 2, 3, 4 and 5mm and their volume fraction satisfy the Rosin-Rammler distribution and are plotted in the figures above.

List of Particles Injected in Post Particle Tracking Process

i	Diameter d_i (mm)	Volume per Bubble in group i (mm^3)	Volume Fraction of Bubble in Group I α_i	Total Volume of Bubbles in Group i (mm^3)	Number of Bubbles in Each Group N_i	Number of Bubbles Injected n_i
1	0.05	6.54E-05	6.40E-09	1.57E-01	2,393	2,393
2	0.075	2.21E-04	2.60E-08	6.36E-01	2,880	2,880
3	0.1	5.24E-04	7.00E-08	1.71E+00	3,272	3,272
4	0.2	4.19E-03	1.54E-06	3.76E+01	8,973	8,973
5	0.3	1.41E-02	6.66E-06	1.63E+02	11,521	11,521
6	1	5.24E-01	1.02E-03	2.49E+04	47,564	4,756
7	2	4.19E+00	1.39E-02	3.39E+05	80,911	8,091
8	3	1.41E+01	3.76E-02	9.19E+05	65,022	6,502
9	4	3.35E+01	2.70E-02	6.61E+05	19,714	1,971
10	5	6.54E+01	3.48E-03	8.52E+04	1,301	1,30
Total	--	--	**0.082**	**2.03E+06**	**243,551**	**51,660**

$n_i = N_i$

$n_i = \frac{N_i}{10}$

- Ni and α_i are calculated based on Rosin-Rammler given in the previous slide.
- The total number of bubbles need to be tracked is about 243,551 which is too large. So, the number of those larger bubbles(1mm to 5mm) are reduced by divide N_i by 10 ($n_i=N_i/10$). The number of small bubbles are kept as $n_i=N_i$.
- In later post processing, the number of tracked large bubbles will be multiply by 10.

How to Compare Simulation Result with Experiment Observation?

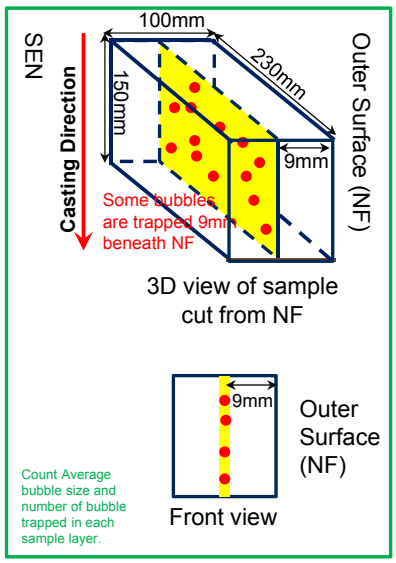

Step1 - Experiment

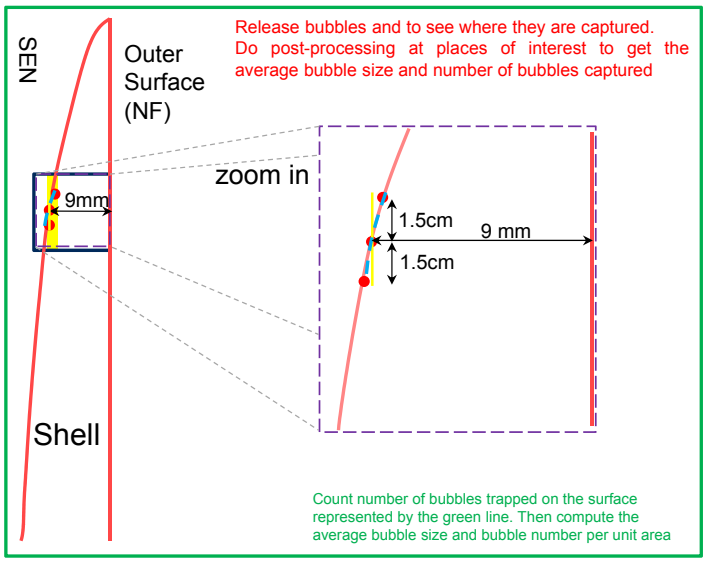

Step 2 – Particles Captured in Simulation

An assumption is that the green dashed line can represent the yellow line.
Similar work can be done on wide surface. The width of the sample equal to the sample width.

How to Compare Simulation Results with Experimental Results

Data available from experiment? ---- Number of bubble captured per 100cm^2 at each experimental sample layer.
Data available from simulations? ---- Number of bubble captured at each simulation sample layer.

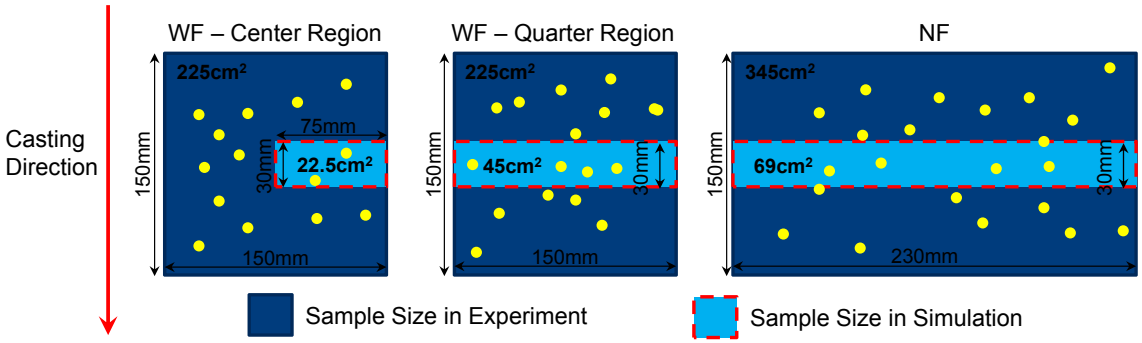

$\bar{N}_E$ number of bubble captured per 100cm in one sampler layer

N_E captured bubble number in a layer of exp. sample

N_e captured bubble number in a layer of exp. sample if the sample is equal to simulation sample size

N_s number of bubble captured in simulation

A_E area of the layer in exp. sample (225cm^2 and 345cm^2 for WF and NF)

A_s area of the layer in simulation sample (22.5cm^2 45cm^2 and 345cm^2 for WF-Center region, WF-Quarter region and NF)

Procedures: $N_E = \bar{N}_E \frac{A_E}{100cm^2}$ → $N_e = N_E \frac{A_s}{A_E}$ → Compare N_e and N_s

Two Different Capture Models

- **Simple capture criterion** (touch=capture) is used at beginning. Particles (bubbles) are captured when they touch NF or WF.

- **Advanced capture criterion** is implemented and the criterion is described both in Quan Yuan's PhD thesis (2004)[7] and Sana Mahmood's Master thesis (2006)[8]. A flow chart of capture criterion is given in figure below. PDAS used in the criterion is obtained from Sana Mahmood's Master thesis (2006)[8] as well.

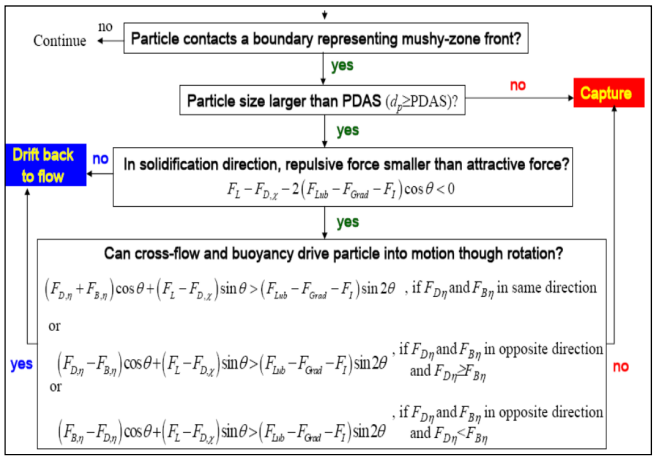

Advanced Capture Criterion (Figure from Sana Mahmood, Master thesis, 2006[8])

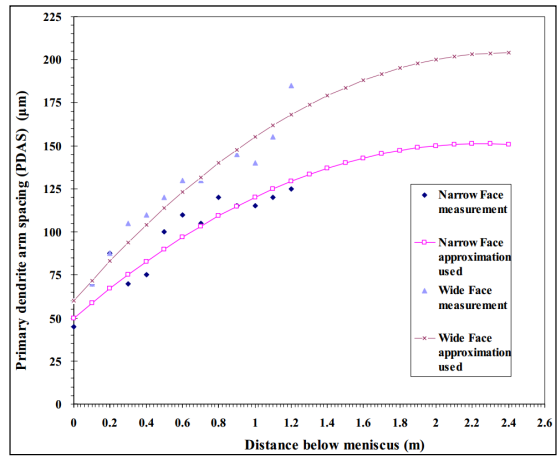

PDAS vs. Distance below meniscus (Figure from Sana Mahmood, Master thesis, 2006[8])

Forces Related to Capture Criterion

R_p particle radius

V_{sol} solidification velocity

r_d dendrite tip radius

h_o distance between dendrite tip and particle

a_o atomic diameter of the liquid

C_o sulfur content of steel

D_s diffusion coefficient of sulfur in steel

k distribution coefficient

Theoretical solidification velocity is used on NF/WF

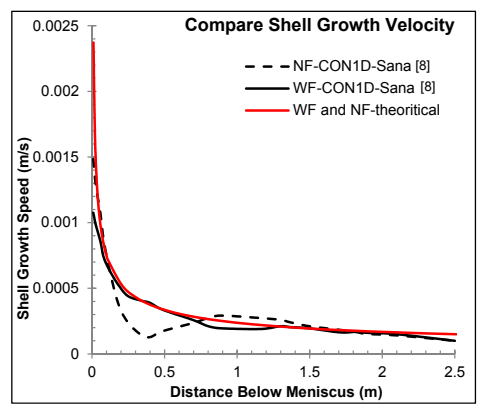

Forces on particles [7,8]:

$$F_B = (\rho_{steel} - \rho_{Ar})\, g \frac{4}{3}\pi R_p^{\,3}$$

Buoyancy force pointing upward

$$F_{\text{lub}} = 6\pi\mu V_{sol} \frac{R_p^{\,2}}{h_o}\left(\frac{r_d}{r_d + R_p}\right)^2$$

Lubrication force acts on the particle along particle's radius towards dendrite tip

$$F_I = 2\pi\Delta\sigma_o \frac{r_d R_p}{r_d + R_p}\frac{a_o^{\,2}}{h_o^{\,2}} \qquad \Delta\sigma_o = \sigma_{sp} - \sigma_{sl} - \sigma_{pl}$$

Van der Waals force pushes particle away from dendrite tip

$$F_{Grad} = -\frac{m\beta\pi R_p}{\xi^2}\left\{\frac{\xi^2 - R_p^{\,2}}{\beta}\ln\frac{(\xi + R_p)\left[\alpha(\xi - R_p) + \beta\right]}{(\xi - R_p)\left[\alpha(\xi + R_p) + \beta\right]}\right\} + \frac{2R_p}{\alpha} - \frac{\beta}{\alpha^2}\ln\frac{\alpha(\xi - R_p) + \beta}{\alpha(\xi + R_p) + \beta}$$

Interfacial gradient force push particle toward solidification front

$$\alpha = 1 + nC_o$$

$$\beta = nr_d\left(C^* - C_o\right)$$

$$\xi = R_p + r_d + h_o$$

$$\frac{r_d V_{sol}}{2D_s} = \frac{C^* - C_o}{C^*(1-k)}$$

Fluid Field Solution
Contour of Velocity Magnitude

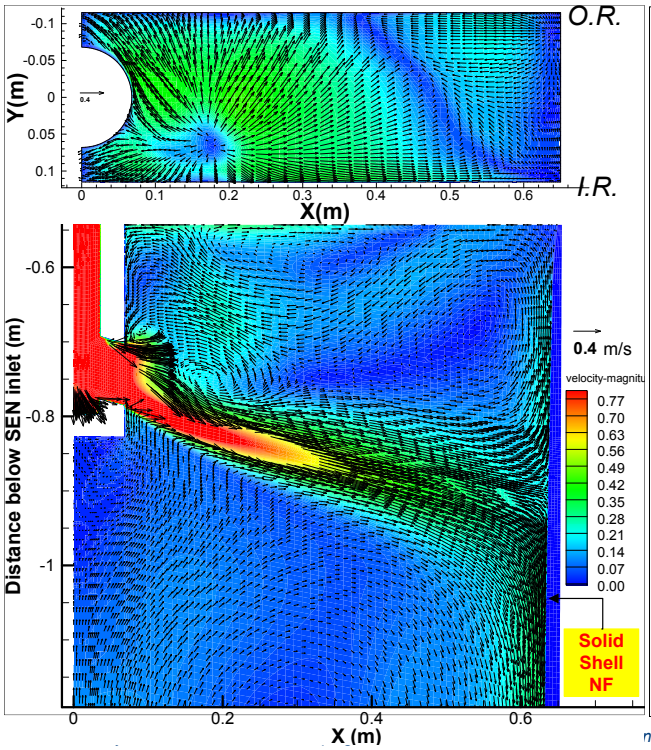

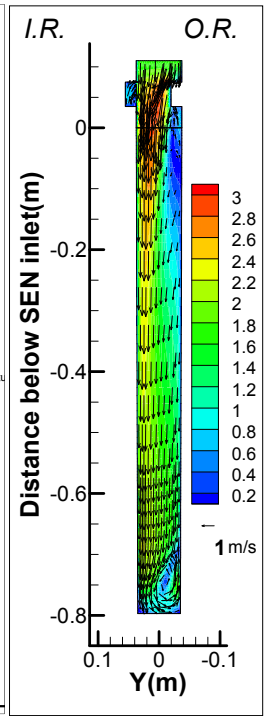

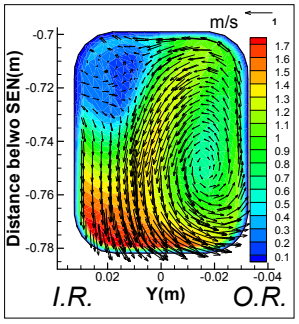

Contour Plot of Velocity Magnitude (m/s)

Left top and Left bottom: meniscus and middle plane

Middle: SEN Symmetric plane

Right: Port (look into SEN)

Velocity at Center line in Meniscus Surface

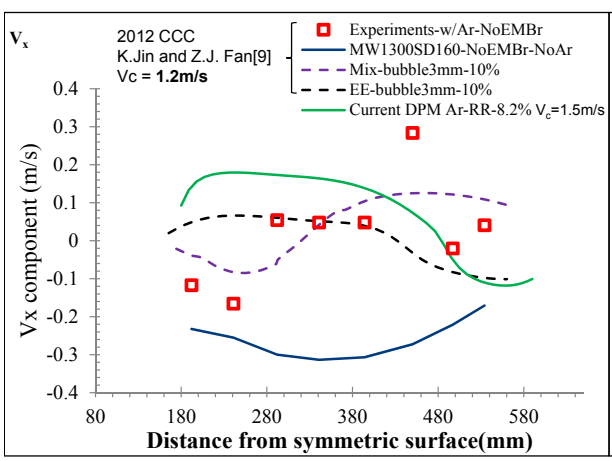

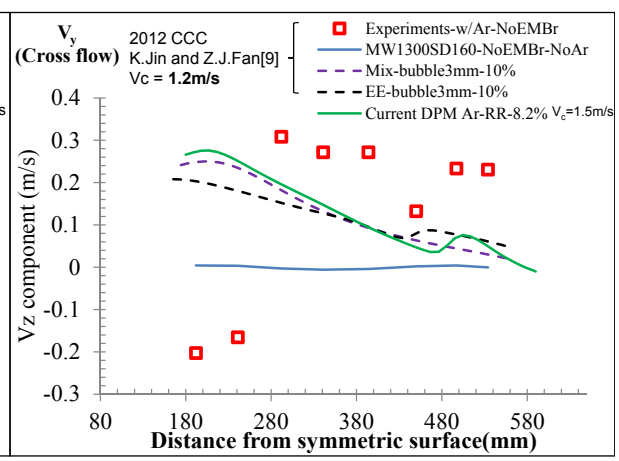

- DPM simulation predict a close shape of V_x but the predicted V_x value is larger than the experiment. Possible reason might be that the casting speed in this simulation is 1.5m/s but in the experiment it was 1.2m/s.
- Regarding the cross flow velocity, all simulations under predict the cross flow speed. The possible reason is the flow is transient but the experimental data is only one snap shot.

Comparison of Velocity at Center line of Meniscus

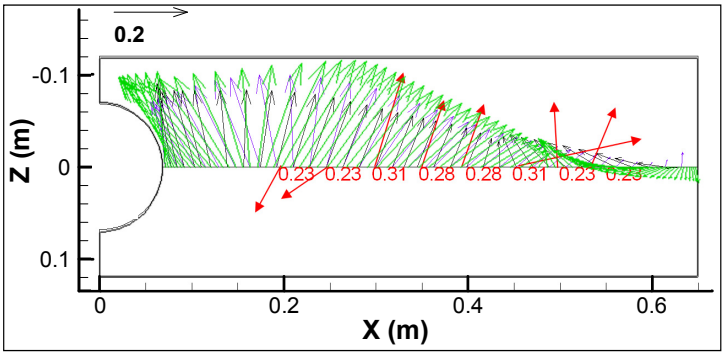

10% Ar, d_p = 3mm, Eulerian Model, Vc = 1.2m/s

10% Ar, d_p = 3mm, Mixture Model, Vc = 1.2m/s

Current Work: 8.2% Ar, Rosin-Ramler with mean d_p = 3mm, Discrete Phase Model, Vc = 1.5m/s

Experiment: with Ar injection ~10%, Vc = 1.2m/s

Red numbers are velocity magnitude obtained from Nailboard test (unit **m/s**)

Increasing casting speed (by 25%) should increase surface velocities(by 25%), which seems to roughly be the case, considering the minor changes due to bubble size differences.

Possible reasons for simulation not matching with the experiments is that the process is transient, but the experiment is only one snapshot.

Study the Effect of Capture Criterion 4 Post Particle Track Are Performed

- 4 post particle track simulations are done.

Particle Number and Size for Post Particle Track Simulations

Case	NO. of bubble Injected	Bubble Size Distribution	Capture Criterion on NF/WF
1	51,660	Constant d_p 1mm	Simple Capture
2	51,660	Constant d_p 1mm	Adv. Capture
3	47,564	Rosin-Rammler, mean d_p 3mm	Simple Capture
4	47,564	Rosin-Rammler, mean d_p 3mm	Adv. Capture

Fluid field solution for the both cases are the same, V_c=*1.5m/s*, Ar gas volume fraction is *8.2%*, all simulations performed on the same grid with ~*1.2* million cells.

Bubbles Captured by NF and WF with Simple Capture Criterion

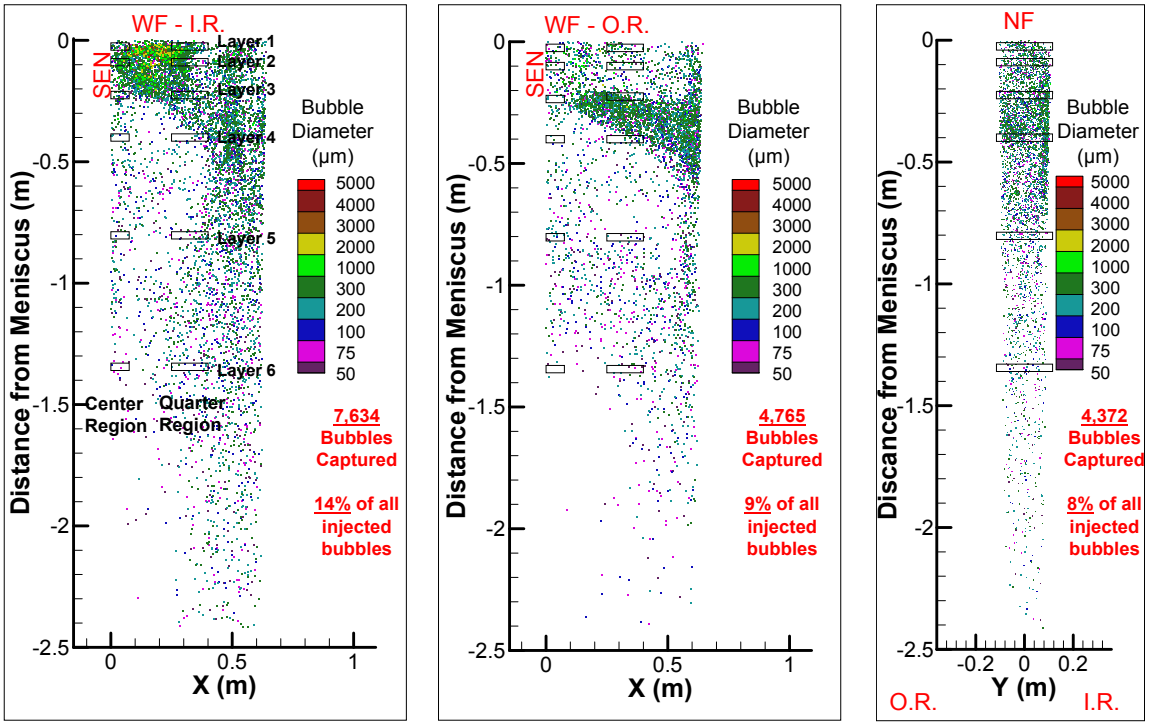

Number of bubbles captured, casting speed 1.5m/min, without EMBr, simple capture criterion

	Layer Location			Simulation Result at WF						Experiment at WF			
	Sample Layer Number	Grind Depth (mm)	Below Meniscus (mm)	Capture bubble N_s and Avg. d_p: I.R. #	I.R. Avg. d_p	O.R. #	O.R. Avg. d_p	Bubble #/100cm² I.R.	Bubble #/100cm² O.R.	Bubbles captured N_E	Bubbles captured N_e	Average d_p (mm)	Bubble #/100cm² $\bar{N}_E$
WF Center Region	1	3	25	29	0.304	6	0.275	129	27	39.2	3.9	0.103	17.4
	2	6	100	72	0.343	6	0.229	320	27	41.0	4.1	0.126	18.2
	3	9	225	19	0.195	7	0.196	84	31	26.8	2.7	0.081	11.9
	4	12	400	4	0.138	2	0.250	18	9	45.2	4.5	0.092	20.1
	5	17	803	2	0.150	6	0.133	9	27	9.5	0.9	0.047	4.2
	6	22	1344	2	0.087	0	0	9	0	0.0	0.0	0	0
WF Quarter Region	1	3	25	119	0.284	27	0.271	264	60	33.3	6.7	0.103	14.8
	2	6	100	128	0.217	14	0.273	284	31	32.9	6.6	0.112	14.6
	3	9	225	71	0.217	109	0.209	158	242	14.2	2.8	0.090	6.3
	4	12	400	15	0.165	20	0.194	33	44	35.1	7.0	0.091	15.6
	5	17	803	13	0.190	8	0.122	29	18	4.7	0.9	0.047	2.1
	6	22	1344	9	0.161	4	0.063	20	9	0.0	0.0	0	0

				Simulation			Experiment			
	Sample Layer Number	Grind Depth (mm)	Below Meniscus (mm)	Captured bubble N_s	Captured bubble Avg. d_p	bubble #/100cm²	bubbles captured N_E	bubbles captured N_e	Average d_p (mm)	bubble #/100cm² $\bar{N}_E$
NF	1	3	25	107	0.221	155	59.0	11.8	0.103	17.1
	2	6	100	134	0.207	194	51.1	10.2	0.072	14.8
	3	9	225	184	0.211	266	42.1	8.4	0.075	12.2
	4	12	400	206	0.198	298	69.7	13.9	0.096	20.2
	5	17	803	54	0.180	78	0.0	0.0	0	0
	6	22	1344	15	0.155	22	16.2	3.2	0.070	4.7

Summary

- Total injected particle is 51,660.
- 4,372 are captured by NF.
- 4,765 are captured by WF – O.R.
- 7,634 are captured by WF – I.R.
- 2,405 are captured by bottom.
- 32,408 escaped from top.
- 76 incomplete

Good trends

Too many entrapped

Bubbles Captured by NF and WF
k-ε Model with Solidification from Theoretical Solution

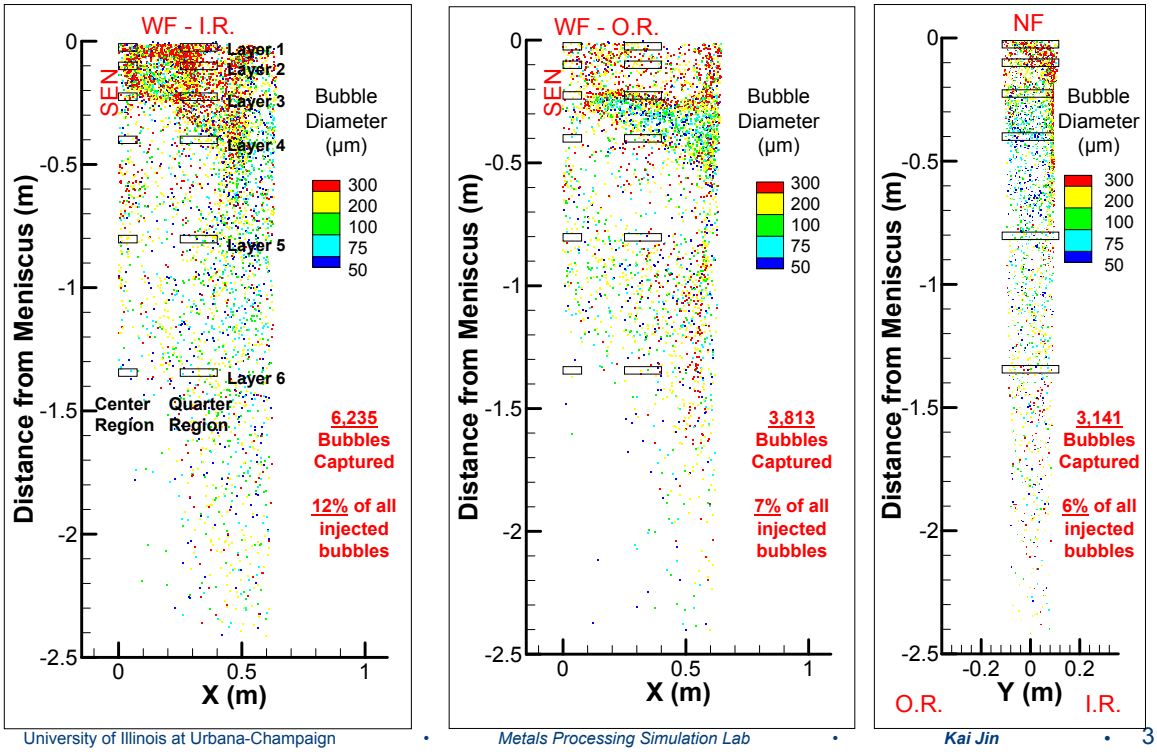

Number of bubbles captured, casting speed 1.5m/min, without EMBr, Adv. capture criterion

	Layer Location			Simulation Result at WF						Experiment at WF			
	Sample Layer Number	Grind Depth (mm)	Below Meniscus (mm)	Capture bubble N_s and Avg. d_p I.R. # & Avg. d_p		O.R. # & Avg. d_p		Bubble #/100cm² I.R.	O.R.	Bubbles captured N_E	N_e	Average d_p (mm)	Bubble #/100cm² $\bar{N}_E$
WF Center Region	1	3	25	37	0.205	9	0.233	164	40	39.2	3.9	0.103	17.4
	2	6	100	57	0.193	10	0.183	253	44	41.0	4.1	0.126	18.2
	3	9	225	17	0.207	4	0.200	75	17	26.8	2.7	0.081	11.9
	4	12	400	6	0.187	1	0.075	26	4	45.2	4.5	0.092	20.1
	5	17	803	6	0.175	0	0	26	0	9.5	0.9	0.047	4.2
	6	22	1344	2	0.075	0	0	8	0	0.0	0.0	0	0
WF Quarter Region	1	3	25	112	0.267	16	0.184	248	35	33.3	6.7	0.103	14.8
	2	6	100	170	0.213	17	0.199	377	37	32.9	6.6	0.112	14.6
	3	9	225	80	0.204	91	0.199	177	202	14.2	2.8	0.090	6.3
	4	12	400	18	0.147	20	0.171	40	44	35.1	7.0	0.091	15.6
	5	17	803	18	0.153	5	0.165	40	11	4.7	0.9	0.047	2.1
	6	22	1344	13	0.152	4	0.163	29	8	0.0	0.0	0	0

				Simulation			Experiment			
	Sample Layer Number	Grind Depth (mm)	Below Meniscus (mm)	Captured bubble N_s	Avg. d_p	bubble #/100cm²	bubbles captured N_E	N_e	Average d_p (mm)	bubble #/100cm² $\bar{N}_E$
NF	1	3	25	170	0.210	246	59.0	11.8	0.103	17.1
	2	6	100	154	0.212	223	51.1	10.2	0.072	14.8
	3	9	225	146	0.184	211	42.1	8.4	0.075	12.2
	4	12	400	78	0.132	113	69.7	13.9	0.096	20.2
	5	17	803	27	0.121	39	0.0	0.0	0	0
	6	22	1344	20	0.185	29	16.2	3.2	0.070	4.7

- 51,660 bubbles are injected
- 6,235 (12%) Captured by WF-IR
- 3,813 (7%) Captured by WF-OR
- 3,141 (6%) Captured by NF
- 34,417 (67%) Escaped from meniscus
- 3,673 (7%)Trapped by bottom
- 381 (1%) Incomplete

Compare Simulation Result with Experiment Result

Experiment
Simple I.R.
Simple O.R.
Advanced I.R.
Advanced O.R.

Simple capture criterion greatly over predict the number of bubble that captured.

Adv. capture criterion predict captured a result is twice larger than the experiment result.

Note: the diameter of the bubble found in experiment of a 2D slice is converted to 3D size following procedure proposed by Simon N. Lekaka, etc. [15]

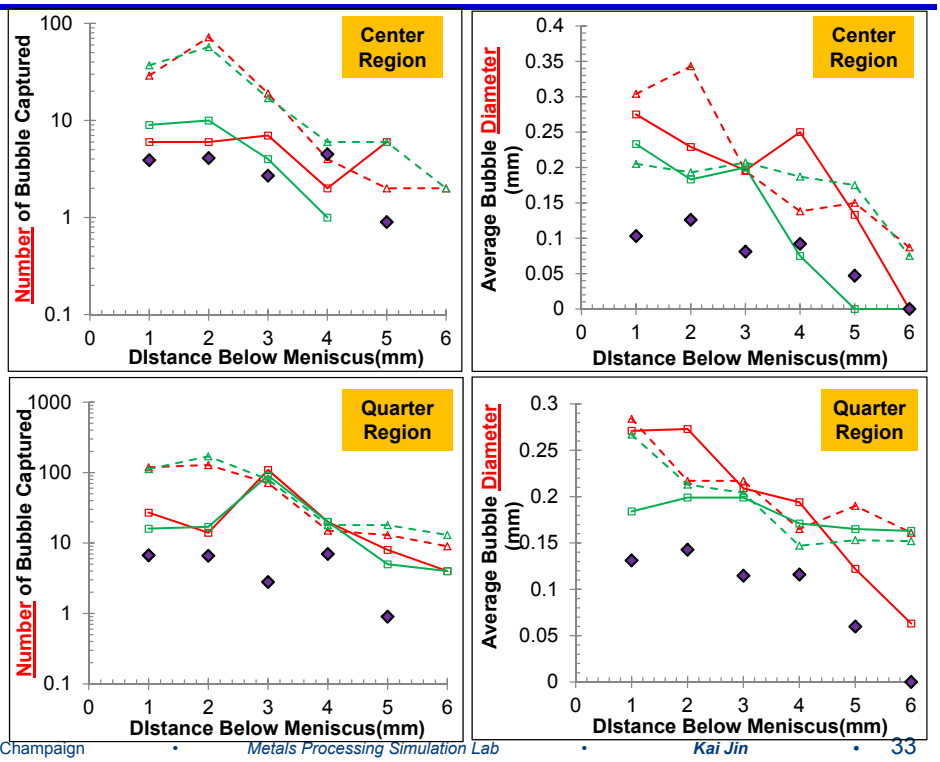

Hook formation: Possible reason for more bubble capture near meniscus

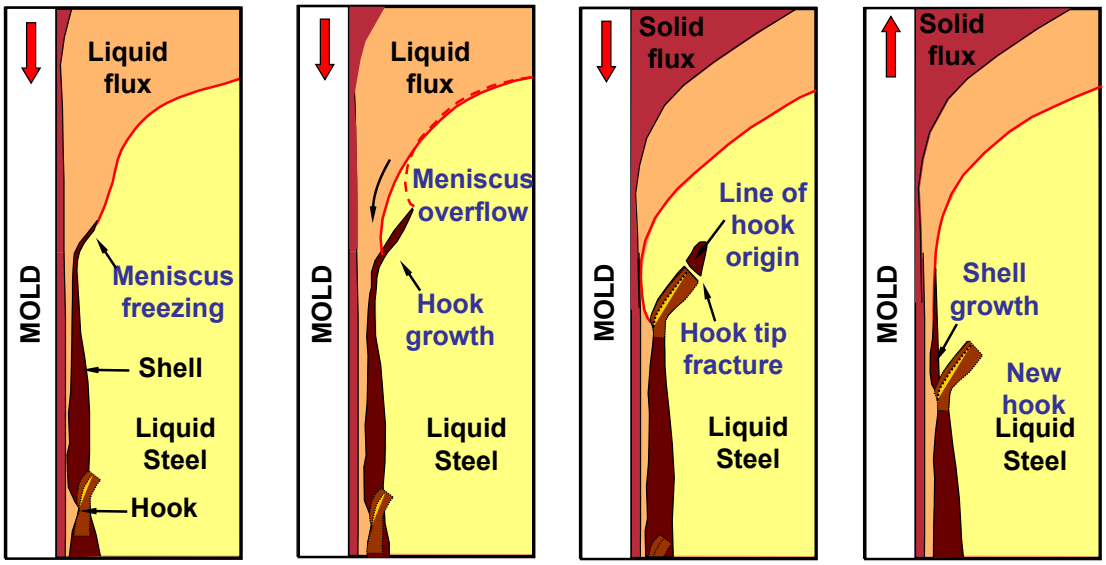

1) Meniscus freezing
2) Meniscus overflow

Level Drop Video

Figures from AK. Thomas & B.G. Thomas, 2010; J. Sengupta, H. Shin, BG Thomas, et al, Met Trans B, 2006

Deep hooks trap particles

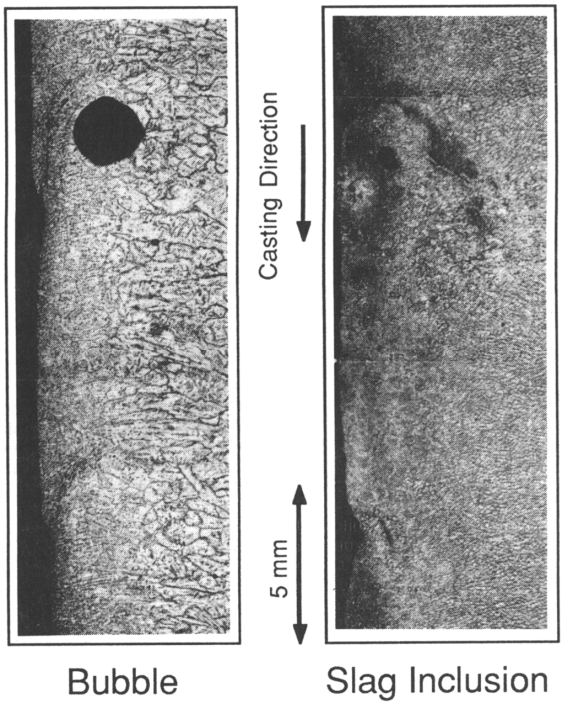

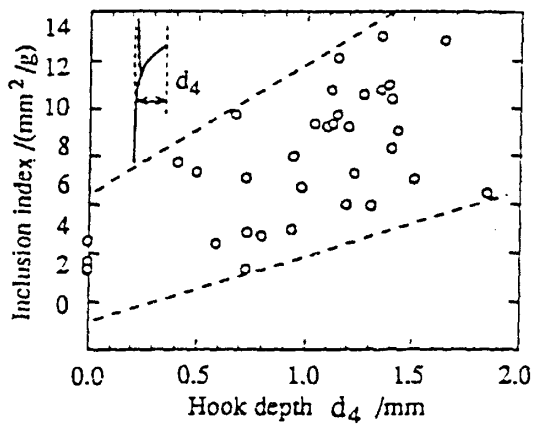

Figure from J.P. Birat et al, IRSID, Malzieres-les-Metz, France, in Mold Operation for Quality and Productivity, ISS, 1991, p.8

Capture of Large Bubbles

- **47,564** bubbles with d_p**=1mm** were injected and a summary of results are listed in the table below. Distribution of captured large bubbles are shown in next two slides.

Criterion	Escaped	d_p (mm)	Captured Bubbles				Incomplete	Capture Rate	# captured large bubble / # captured bubble total
			Total	NF	WF-IR	WF-OR			
Simple	44,760	1	2,749	201	2004	544	55	**0.09%**	$\frac{2749}{19,520}$ = **14%**
Adv.	47,499	1	43	8	33	2	22	**6%**	$\frac{43}{13,232}$ = **0.3%**

- Relative Capture Rate: plant measurement[6] shows that the captured large bubbles (d_p>*1mm*) is ***0.5%*** (2 bubbles out of all bubbles).

compare simulation with measurement

- Large bubble capture location: plant measurement[6] shows the distance of captured large bubbles are within 2mm from the outer surface which is no more than **1cm** below meniscus. Advanced capture criterion also predict large bubbles got captured at the very top of the meniscus.

Large Bubbles(d_p=1mm) Captured by NF and WF with Simple Capture Criterion

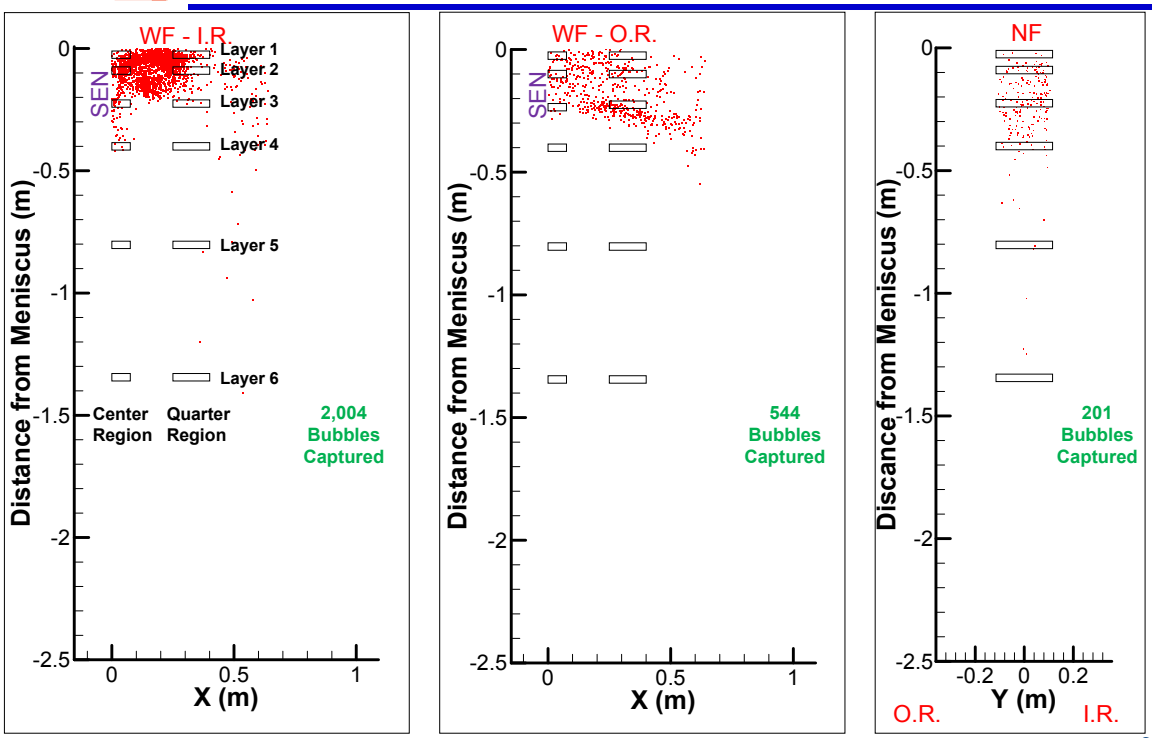

Large Bubbles(d_p=1mm) Captured by NF and WF with Advanced Capture Criterion

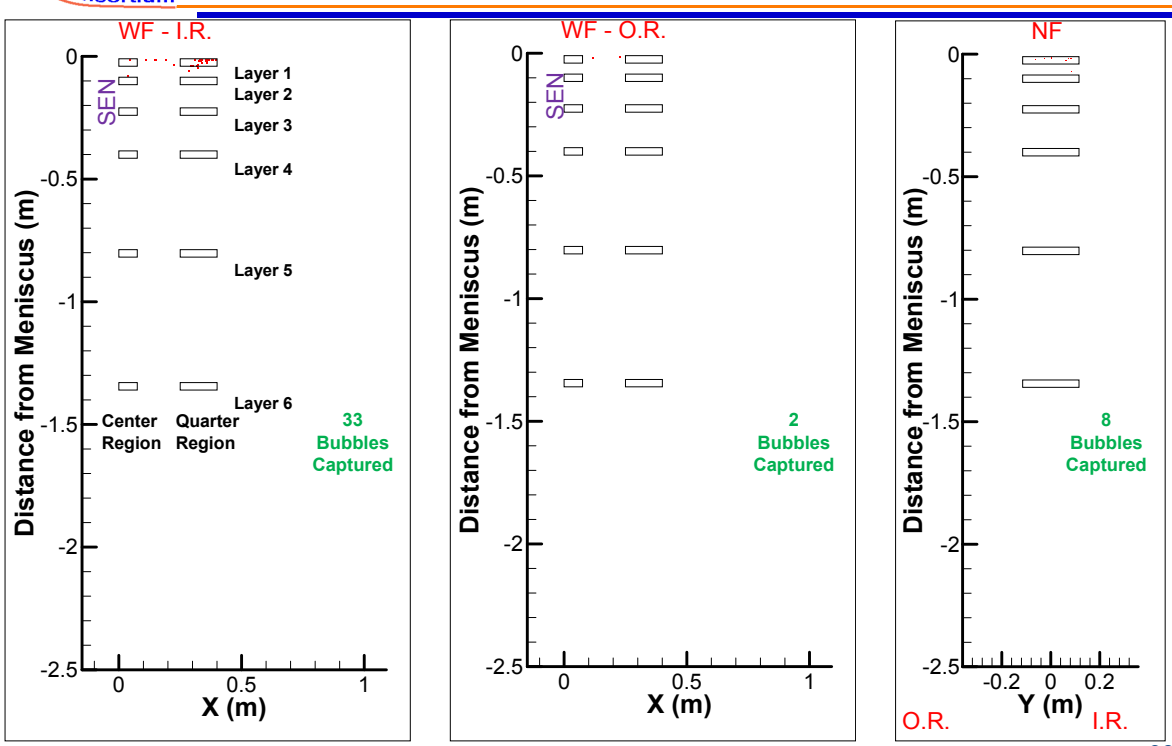

Conclusions

- The DPM simulation predicts similar fluid flow behavior in meniscus region as Eulerian/Mixture simulation that the 8%~10% Ar injection result in cross-flow in meniscus region; when compared with experiment, all these models underpredict the cross flow observed in Baosteel nailboard experiment. Possible reasons are that 1) the experiments are only rare snap shots of this transient process or 2) some other problems are occurring in the plant to cause the asymmetric flow, which are not included in the model;

- Simple capture criterion greatly (3 to 20 times) overpredicts the small argon bubbles trapped in the NF and WF shell; this demonstrates the large frequency of particles that touch the dendritic interface, and are washed away without being captured;

- Advanced capture criterion generally predicts similar number of bubbles trapped by WF as experiment measurements. However, it's slightly over predict the number of bubble captured at some region. Possible reason is k-ε model assumes isotropic turbulence which is not true at near wall region. The k-ε model overpredicts the number of bubbles that penetrate into the boundary layer. More bubbles are trapped by I.R. at region close to SEN; more bubbles are trapped by O.R. at region close to NF. This is likely due to the biased-flow effect of the slide gate on the swirling jet exiting the SEN ports, the captured Ar bubbles are not symmetric;

- The advanced capture criterion correctly predicts that bubbles larger then 1mm diameter are very difficult to be captured (capture rate less than 0.1%) and correctly predicted the location of where those large bubbles will be captured. The bubble sizes predicted by this criterion generally match the measurements, and the observed trend of decreasing size with distance below meniscus is also matched.

Chapter 3

Parametric Study

Casting Conditions, Boundary Conditions and Material Properties

Casting Conditions	Value
Mold Thickness	230 mm
Mold Width	1300 mm
Submergence Depth	160/220 mm
Port Downward Angle	15/25 deg.
Casting Speed	1.5 m/min

Properties	Steel	Ar
Density (kg/m^3)	7,000	0.5
Viscosity (kg/m-s)	0.0063	2.12e-5
Electrical Conductivity (S/m)	714,000 [3]	1.0e-15 [4]
Magnetic Permeability (h/m)	$1.26*10^{-6}$ [3]	$4\pi*10^{-7}$

Location	Boundary Condition
Inlet	V = 1.69 m/s
Outlet	Pressure 184kpa
Symmetry Plane	Symmetry
Top Surface (Meniscus)	No-slip wall; particle can escape;
NF and WF	No-slip wall; with steel mass & momentum sink; particle reflect
Other Places	No-slip wall; particle reflect;

Simulations

Using Discrete Phase model.

Simulation No.	Mold Width (mm)	Nozzle Downward Angle (º)	Submergence Depth (mm)	Ar Gas Conditions (Mean Diameter, Volume Fraction)	EMBr Conditions (Amp)
1	230	15	165	No Ar Injection	No EMBr
2	230	15	165	No Ar Injection	T400B600
3	230	15	165	3mm, 8.2%	No EMBr
4	230	15	165	3mm, 8.2%	T400 B600**
5	230	15	210	3mm, 8.2%	No EMBr
6	230	25	165	3mm, 8.2%	No EMBr
7	230	25	165	3mm, 8.2%	T400 B600
8	230	25	210	3mm, 8.2%	T400 B600
9	230	15	165	3mm,16.4%	No EMBr
10	240	15	165	3mm, 8.2%	No EMBr

NOTE: 3mm means that the average bubble size is 3mm (not mean all bubble with constant diameter) bubble size distribution is Rosin-Rammler.

DPM Settings

- Flow Rate of Ar $1.67*10^{-4}$ kg/s
- Rosin-Rammler Distribution:
  - Min. Diameter(mm): 1
  - Max. Diameter(mm): 5
  - Mean Diameter(mm): 3
  - Shape Parameter: 3.5
- Ar Volume Fraction 8.2%

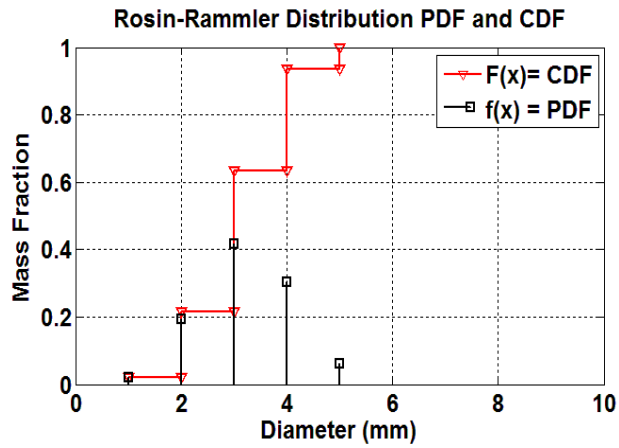

$$R_{Vs} = WHV_c = 1.3m \times 0.23m \times 1.5m / \min = 0.449m^3 / \min$$

$$R_{VAr} = \frac{R_{Vs} Vo_{Ar}}{Vo_s} = \frac{0.449 \times 0.082}{0.918} = 0.04m^3 / \min = 6.7 \times 10^{-4} m^3 / s$$

$$R_{MAr} = \rho_{Ar} R_{VAr} = 0.5kg / m^3 \times 6.7 \times 10^{-4} m^3 / s = 3.33 \times 10^{-4} kg / s$$

Since only one have of the caster: $1.67 \times 10^{-4} kg / s$

$$F(x) = 1 - \exp\left[-\left(\frac{x}{\bar{x}}\right)^b\right]$$

$F(x)$ = cumulative mass % retained on size x

$\bar{x}$ = size parameter b = shapre parameter

Velocity at Center line and 1cm beneath Meniscus

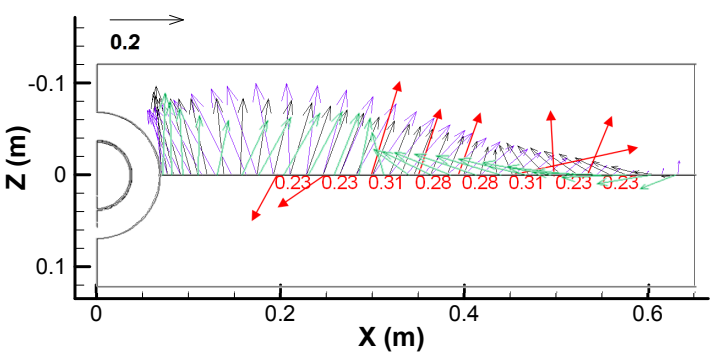

Ar-bubble-3mm-10%-NoEMBr Eulerian Model

Ar-bubble-3mm-10%-NoEMBr Mixture Model

Experiment-w/Ar-NoEMBr

Red numbers are velocity magnitude obtained from Nailboard test (unit m/s)

Cyan arrows are the result of case 10 (casting speed 1.5m/min, Rosin-Rammlar bubble distribution with mean diameter 3mm).

Why not quite matching with experiment?
A possible reason is that only one measurement is available, but the flow in the mold is really a transient turbulent flow. The measurement is only a snapshot of the whole transient process, so it's really hard to match with that experiment.

Effect of EMBr

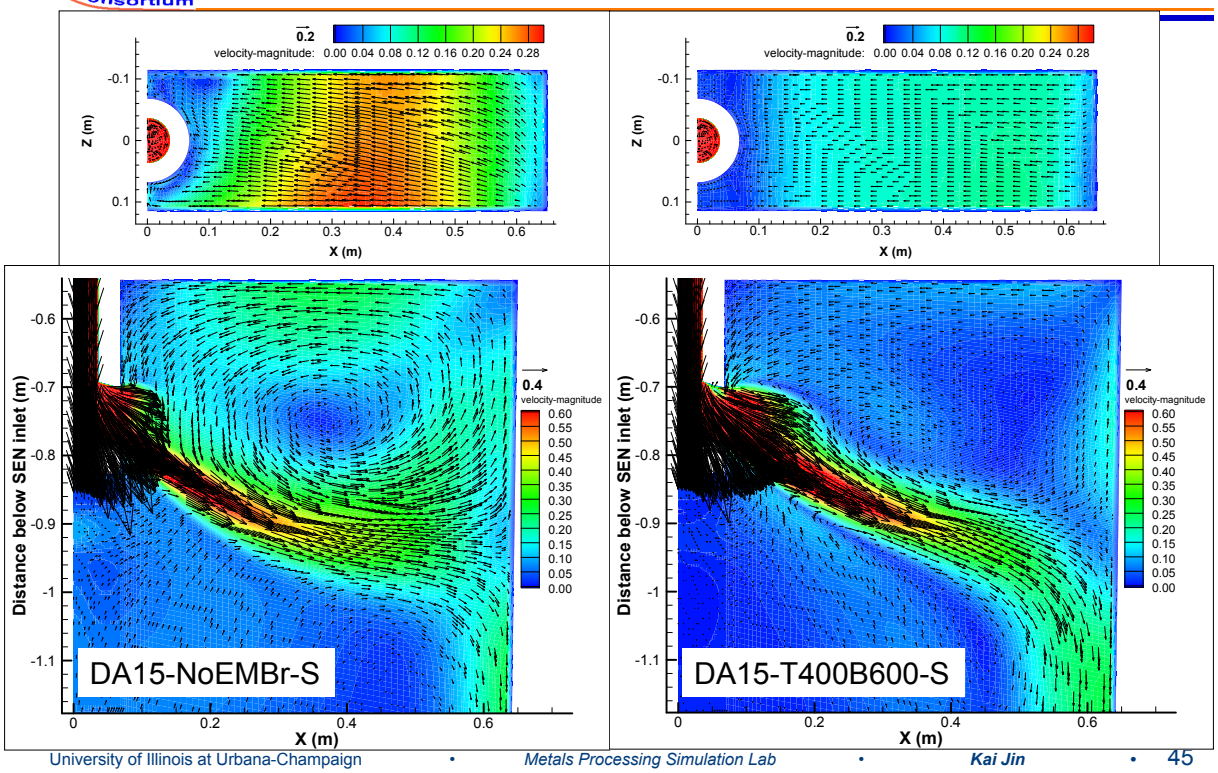

Effect of Ar Injection

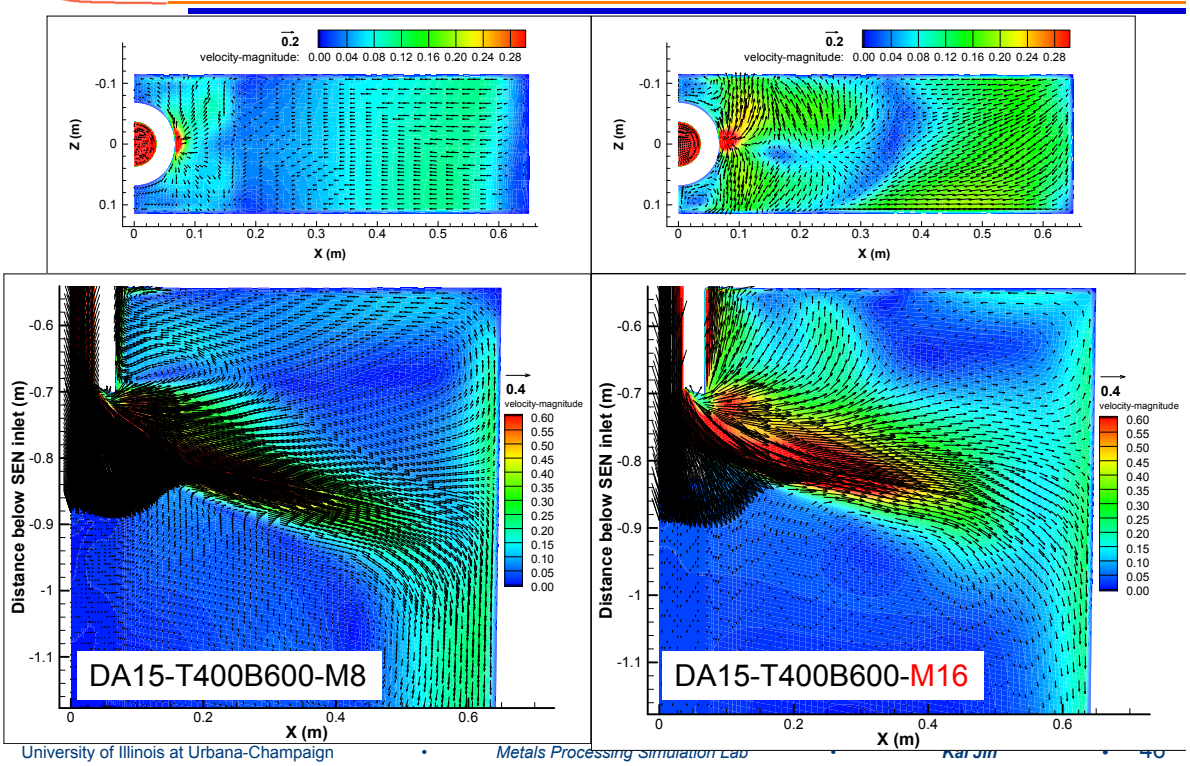

Effect of SEN Downward Angle

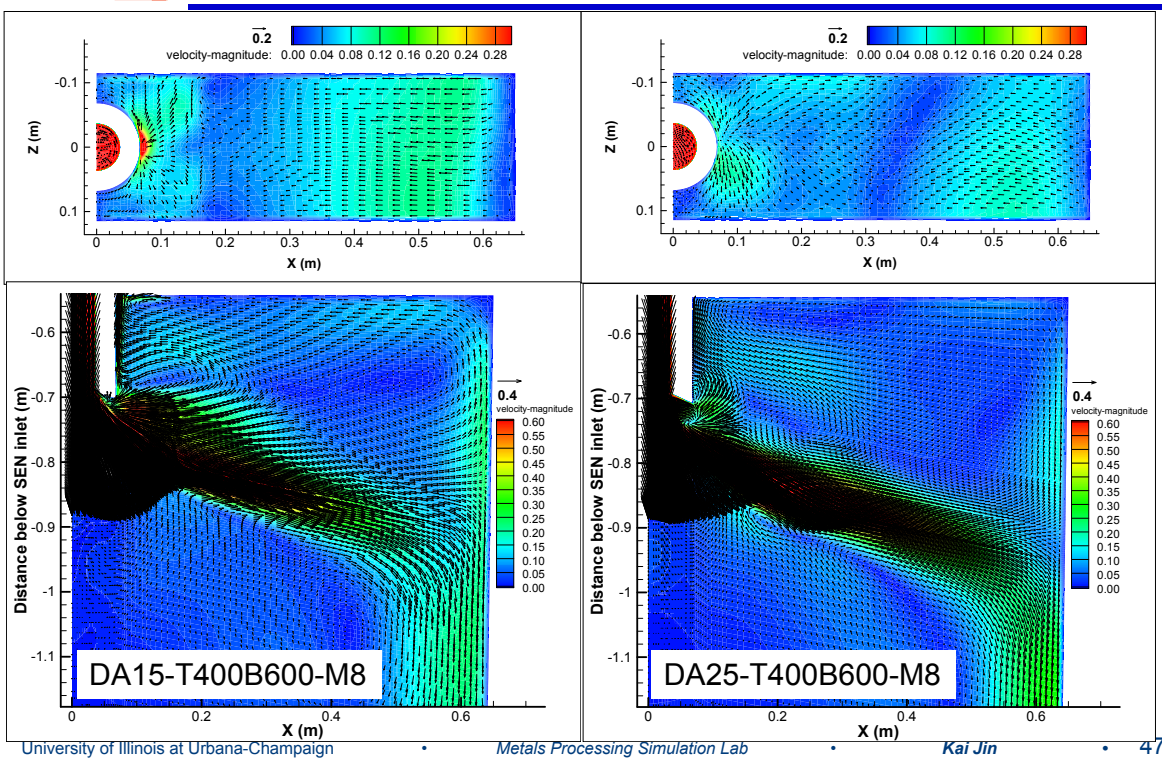

Conclusions

- The Eulerian-Lagrangian method is able to predict the flow pattern including cross flow in the caster. But similar to the previous Eulerian and Mixture simulation, it cannot match exactly with the instantaneous plant measurements.(likely cause is too much variation between plant experiments – snapshots, and average behavior that is modeled)
- Top surface velocity can be increased by:
  1) Reducing SEN downward angle;
  2) Turning off EMBr (upper ruler of FC mold);
  3) Decreasing submergence depth;
  4) Increasing Ar volume fraction (side effect of causing cross flow)
- By turning off the EMBr the maximum velocity on the top surface increases from 0.16 m/s to 0.3m/s which means that the top surface velocity can be increased by as much as 85%. The puts top surface velocity in 0.2-0.4 m/s range, so should be good for steel quality.[6]
- Regarding the effect of SEN downward angle, the simulations indicate that decreasing the SEN downward angle can help increasing the surface velocity. Under the condition that downward angle 25° and casting speed 1.5 m/s with EMBr T400B600, reducing the downward angle from 25° to 15° can cause the top surface velocity increase from 0.1m/s to 0.16m/s which correspond to a 60% increment.

Future Work

- Current *k-ε* model with random walk tracking cannot accurately predict the particle motion when they come to the vicinity of wall, hence more accurate model (LES) may be implemented in the future;

- Recent studies[16] on particle-solidification front interactions shows that whether a particle/bubble can be captured by solidification front also greatly depend on the thermal conductivity of the particle and the solidifying medium, this dependence can be included in the future;

- The formula of lubrication force used in the advanced capture criterion was derived from spherical particle interact with planar solidifying front which may not be accurate in dendritic front case, the formula of this force might be improved;

References

[1] Ansys, Inc, ANSYS WORKBENCH and ICEMCFD Manual.

[2] Rui Liu, GroupMeeting Sep.26, 2011, R. Liu *Shell and Particle*.

[3] Yu Haiqi, Wang Baofeng, Li Huiqin, Li Jianchao, *Influence of electromagnetic brake on flow field of liquid steel in the slab continuous casting mold*, Journal of Materials Processing Technology, Volume 202, Issues 1–3

[4] S. D. Pawar, P. Murugavel, D. M. Lal, *Effect of relative humidity and sea level pressure on electrical conductivity of air over Indian Ocean*, Journal of Geophysical Research, vol. 114, D02205, 8 PP., 2009

[5] Hua Bai and Brian G. Thomas, Effects of clogging, argon injection, and continuous casting conditions on flow and air aspiration in submerged entry nozzles, METALLURGICAL AND MATERIALS TRANSACTIONS B, Volume 32, Number 4 (2001), 707-722, DOI: 10.1007/s11663-001-0125-4

[6] Baosteel Bubble Summary Report

[7] Quan Yuan, "*Transient Study of Turbulent Flow and Particle Transport during Continuous Casting of Steel Slabs*," PhD Thesis, University of Illinois, June, 2004.

[8] Sana Mahmood, "*Modeling of Flow Asymmetries and Particle Entrapment in Nozzle and Mold During Continuous Casting of Steel Slabs*", MS Thesis, University of Illinois, 2006

[9] Kai Jin and Zhengjie Fan, "*Mold Flow with Argon Gas, EMBr and Evaluation using Nailboard Measurements*" Report No. CCC201205, University of Illinois at UrbanaChampaign, 2012

[10] J. Kubota, K. Okimoto, A. Shirayama, and H. Murakami: Steelmaking Conf. Proc., Iron and Steel Society, Warrendale, PA, 1991, vol. 74, pp. 233–41

[11] Thomas, Brian G., A. Denissov, and Hua Bai. "*Behavior of argon bubbles during continuous casting of steel.*" *Steelmaking Conference Proceedings*. Vol. 80. IRON AND STEEL SOCIETY OF AIME, 1997.

[12] 2007 Kevin Cukierski MS Thesis, *Electromagnetic Flow Control In The Continuous Casting Of Steel Slabs*

[13] M.J. Cho, I.C. Kim, S.J. Kim, and J.K. Kim:Trans. KSME, 1999, vol. 23B(13), pp. 1491–1502

[14] Thomas, Brian G., A. Denissov, and Hua Bai. "*Behavior of argon bubbles during continuous casting of steel.*" *Steelmaking Conference Proceedings*. Vol. 80. IRON AND STEEL SOCIETY OF AIME, 1997

[15] Simon N. Lekakh, Vivek Thapliyal and Kent Peaslee, *"Use of an Inverse Algorithm for 2D to 3D Particle Size Conversion and Its Application to Non-Metallic Inclusion Analysis In Steel*", PR-364-102 - 2013 AISTech Conference Proceedings

[16]Garvin, J. W., and H. S. Udaykumar. "Drag on a particle being pushed by a solidification front and its dependence on thermal conductivities." *Journal of crystal growth* 267.3 (2004): 724-737.

Acknowledgments

- Continuous Casting Consortium Members (ABB, ArcelorMittal, Baosteel, Magnesita Refractories, Nippon Steel and Sumitomo Metal Corp., Nucor Steel, Postech/ Posco, Severstal, SSAB, Tata Steel, ANSYS/ Fluent)
- Baosteel (Prediction Measurement and Optimization of Mold Fluid Flow in Continuous Slab Casting with FC Mold at Baosteel, UIUC Research Project 2011-03313 C5241)
- Baosteel (plant data, including geometry, nailboard measurements, SVC measurements, particle measurements)
- ABB (EMBr magnetic field data)